A Topological Study of the Transition States of the Hydrogen Exchange and Dehydrogenation Reactions of Ethane on a Zeolite Cluster

N. B. Okulik

Departamento de Química, Facultad de Agroindustrias, UNNE, Cte. Fernández 755, 3700 Sáenz Peña, Chaco, Argentina

R. Pis Diez*,† and A. H. Jubert†,‡

CEQUINOR, Centro de Química Inorgánica (CONICET-UNLP), Departamento de Química, Facultad de Ciencias Exactas, UNLP, C.C. 962, B1900AVV La Plata, Argentina and Facultad de Ingeniería, UNLP, 1900 La Plata, Argentina

Received: October 17, 2003; In Final Form: February 6, 2004

The transition states of the hydrogen exchange and dehydrogenation reactions of ethane on a zeolite acid site are calculated using the density functional theory and analyzed with the atoms-in-molecules method. The transition state for the hydrogen exchange reaction is characterized by a slightly ionic interaction between a distorted H-ethonium structure, $C_2H_7^+$, and a negatively charged zeolite cluster. No free carbocation is found. The dehydrogenation reaction, on the other hand, shows a transition state with three well-defined fragments, namely, an ethyl cation, $C_2H_5^+$, a negatively charged zeolite cluster, and a H_2 pseudomolecule, in which the H−H bond is somewhat larger than the equilibrium value in H_2. The interaction between those fragments can be described as a closed-shell one, typical of rather ionic systems.

Introduction

Acid-catalyzed processes, such as cracking, hydrogen exchange, and dehydrogenation, are industrial transformations of high economic importance.[1,2] Zeolites are among the most employed acid catalysts in such transformation processes. Furthermore, acid-catalyzed reactions share one common feature, namely, they involve hydrocarbons. When a given hydrocarbon interacts with a zeolite acid site (ZOH), either a hydrogen exchange reaction (equation 1 below) or a dehydrogenation process (equation 2) can occur

$$\mathrm{ZOH^* + C_nH_{2n+2} \rightarrow ZOH + H^*C_nH_{2n+1}} \quad (1)$$

$$\mathrm{ZOH + C_nH_{2n+2} \rightarrow ZOC_nH_{2n+1} + H_2} \quad (2)$$

The suggested mechanism for the above reactions proposes the participation of carbocations as intermediates.[3] The initial step in the formation of those carbocations is often ascribed to a proton attack on a C−H or C−C bond,[4] following the concept of σ-basicity developed by Olah in the framework of extensive investigation of electrophilic reactions on single bonds in superacidic media.[5]

The existence of carbocations as intermediates in reactions over zeolites and superacidic media has been proved experimentally.[6] Unfortunately, characterizing those protonated species using spectroscopic techniques is a difficult task to accomplish. This fact reveals the importance of using theoretical tools in the study of those processes to complement experimental efforts.

Theoretical methods have been widely employed to study zeolite-catalyzed reactions. Because of the complex structure of zeolites, most of the theoretical work is performed considering a cluster model to represent part of the structure. One such model is the T3 cluster formed by three tetrahedral units, where T stands for Al or Si. Several reactions have been studied using the T3 cluster with the aim of understanding both the formation and the nature of intermediates and transition states when small hydrocarbons interact with a zeolite acid site.[7,8]

The hydrogen exchange reaction of ethane on a zeolite acid site has already been investigated by some groups using different theoretical approaches[7,9] (see also 10 and references therein). Blaszkowski and co-workers carry out local density calculations within the framework of the density functional theory with a double-ζ plus polarization basis set.[9] The authors include density gradient corrections in a perturbative manner to attain more accurate binding energies. Esteves et al., on the other hand, use the B3LYP and MP2 methods with a 6-31G** basis set to investigate the reaction.[7] Both studies clearly suggest that no free carbocation is formed as intermediate in the reaction. Moreover, these studies show that the transition state found for the hydrogen exchange reaction of ethane on a zeolite acid is characterized by a $C_2H_7^+$ carbocation, in which one carbon atom is coordinated to four hydrogen atoms.

No theoretical studies exist, to our knowledge, on the dehydrogenation reaction of ethane on a zeolite acid site.

In a recent work, a topological study of the transition states of the hydrogen exchange and dehydrogenation reactions of methane on a zeolite acid site was presented by us.[8] As a further contribution to the understanding of how small hydrocarbons interact with zeolites, the nature of the transition states formed when ethane reacts with a T3 cluster is investigated in the present work within the framework of the density functional theory[11] and further analyzed using the atoms-in-molecules method.[12]

* Corresponding author. E-mail address: pis_diez@quimica.unlp.edu.ar.
† CEQUINOR.
‡ FI, UNLP.

10.1021/jp037149s CCC: $27.50
Published on Web 03/09/2004

Method and Calculation Details

The transition states (TS) for the hydrogen exchange and dehydrogenation reactions of ethane on a zeolite cluster are calculated using the density functional theory[11] and their topological properties are analyzed in terms of the atoms-in-molecules method.[12]

Geometry optimizations and vibrational frequency calculations are carried out using the Gaussian 94 package.[13] The Becke's three-parameter density functional[14] together with the Lee, Yang, and Parr functional, which accounts for both local and gradient-corrected correlation effects,[15] are used to accomplish the calculations. This combination leads to the well-known and widely used B3LYP method. The basis set used throughout the work is 6-31G**.

The zeolite acid site is represented by a linear T3 cluster (T = Si, Al) in which the mid tetrahedron contains the Al atom. The OH groups attached to the silicon atoms in the terminal tetrahedrons are replaced by hydrogen atoms to diminish the computational effort. Ethane does not interact with such terminal groups when it approaches the T3 cluster; thus, the above substitution should not affect the quality of the results.

All the structures needed for the present study are optimized without constraints. These systems are confirmed as true minima by the presence of real harmonic frequencies after the corresponding vibrational analysis. The TS for the hydrogen exchange and dehydrogenation reactions of ethane on the T3 system are optimized using the eigenvector method[16] and they are characterized as first-order saddle points by the presence of one and only one imaginary harmonic vibrational frequency.

The topological analysis of all the species under study is accomplished by means of the PROAIM program.[17] The densities used for the topological analysis are obtained through single-point calculations on the above optimized geometries and transition states using the B3LYP level of theory and the 6-311++G** basis set provided by the Gaussian 94 package.

Atoms-In-Molecules Theory: An Overview. The atoms-in-molecules theory is a simple, rigorous, and elegant way of defining atoms and bonds within a chemical structure. This theory is based on the critical points (CP) of the electronic density, $\rho(\mathbf{r})$. These are points where the gradient of the electronic density, $\nabla\rho(\mathbf{r})$, vanishes and are characterized by the three eigenvalues (λ_1, λ_2, λ_3) of the Hessian matrix of $\rho(\mathbf{r})$. The CPs are labeled as (r, s) according to their rank, r (number of nonzero eigenvalues), and signature, s (the algebraic sum of the signs of the eigenvalues).

Four types of CPs are of interest in molecules: (3, −3), (3, −1), (3, +1), and (3, +3). A (3, −3) point corresponds to a maximum in $\rho(\mathbf{r})$ and occurs generally at the nuclear positions. A (3, +3) point indicates electronic charge depletion and is known as cage critical point. (3, +1) points, or ring critical points, are merely saddle points. Finally, a (3, −1) point, or bond critical point, is generally found between two neighboring nuclei indicating the existence of a bond between them.

Several properties that can be evaluated at a bond critical point (BCP) constitute very powerful tools to classify the interactions between two fragments.[12] The two negative eigenvalues of the Hessian matrix (λ_1 and λ_2) at the BCP measure the degree of contraction of $\rho(\mathbf{r})$ perpendicular to the bond toward the critical point, while the positive eigenvalue (λ_3) measures the degree of contraction parallel to the bond and from the BCP toward each of the neighboring nuclei. When the negative eigenvalues dominate, the electronic charge is locally concentrated in the region of the BCP leading to an interaction typically found in covalent or polarized bonds and being characterized by large $\rho(\mathbf{r})$ values, $\nabla^2\rho(\mathbf{r}) < 0$, $|\lambda_1|/\lambda_3 > 1$, and $G/\rho(\mathbf{r}) < 1$, G being the local kinetic energy density at the BCP, which is defined in atomic units as[12]

$$G = \frac{N}{2}\int \nabla\Psi^*(\mathbf{r},\mathbf{r}',\mathbf{r}'',...)\nabla\Psi(\mathbf{r},\mathbf{r}',\mathbf{r}'',...)\, d\mathbf{r}'\, d\mathbf{r}''... \quad (3)$$

where N is the number of electrons in the system. It is evident from the above equation that G depends on $\mathbf{r}$.

If the positive eigenvalue is dominant, on the other hand, the electronic density is locally concentrated at each atomic site. The interaction is now referred to as a closed-shell one and it is characteristic of highly ionic bonds, hydrogen bonds, and van der Waals interactions. Its main features are relatively small $\rho(\mathbf{r})$ values, $\nabla^2\rho(\mathbf{r}) > 0$, $|\lambda_1|/\lambda_3 < 1$, and $G/\rho(\mathbf{r}) > 1$. Finally, the ellipticity, ϵ, defined as $\lambda_1/\lambda_2 - 1$ indicates the deviation of the electronic charge density from the axial symmetry of a chemical bond providing a quantitative measure of the π character of the bond. Large ϵ values indicate that the bond under study has an intrinsic instability and will tend to undergo a distortion to relax to a stable form.[18]

Most of the properties discussed above are presented in the following table for clarity and pedagogical issues.

covalent or shared interactions	ionic or closed-shell interactions
large values of $\rho(\mathbf{r})$	small values of $\rho(\mathbf{r})$
$\nabla^2\rho(\mathbf{r}) < 0$	$\nabla^2\rho(\mathbf{r}) > 0$
$\lvert\lambda_1\rvert/\lambda_3 > 1$	$\lvert\lambda_1\rvert/\lambda_3 < 1$
$G/\rho(\mathbf{r}) < 1$	$G/\rho(\mathbf{r}) > 1$

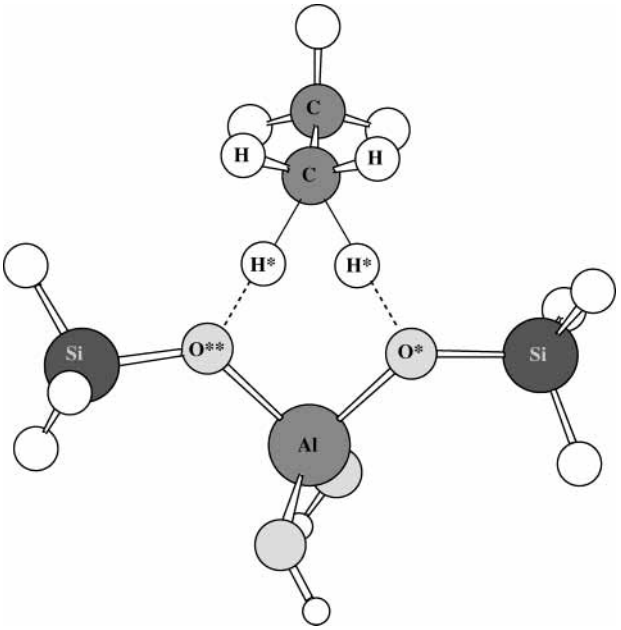

Figure 1. Optimized geometry of the transition state for the hydrogen exchange reaction of ethane on a T3 cluster. See Tables 1 and 2 for labels.

Results and Discussion

Figure 1 shows the optimized geometry of the TS for the hydrogen exchange reaction of ethane on a T3 cluster representing a zeolite acid site. The most relevant geometric parameters of C_2H_6, $C_2H_7^+$, T3, and TS are listed in Table 1.

It can be seen from the figure that the TS seems to be formed by the interaction of a negatively charged T3 fragment and a free $C_2H_7^+$ ion, which arises when ethane is protonated at a C−H bond and is termed H-ethonium. The comparison of some

TABLE 1: Selected Bond Lengths (*r*, in Å) and Bond Angles (α, in Degrees) of Optimized Geometries of T3, C_2H_6, $C_2H_7^+$, and TS for the Hydrogen Exchange Reaction of Ethane on T3 (1) and of $C_2H_5^+$ and TS for the Dehydrogenation Reaction of Ethane on T3 (2)

parameter	T3	C_2H_6	$C_2H_7^+$	TS (1)	$C_2H_5^+$	TS (2)
r(C−H)		1.095	1.092	1.097	1.090	1.090
r(C−C)		1.529	1.517	1.531	1.383	1.470
r(C−H*)			1.206	1.316	1.320	1.791[a]
r(C−O*)						2.761
r(C−O**)						2.443
r(O*−H*)	0.964			1.356[b]		1.886
α (C−H*−C)					58.4	
α (H−C−H)		107.5	104.1	103.3	118.5	117.8
α (H*−C−H*)			44.1	63.1		70.1

[a] This value corresponds to the shorter C−H* bond, which is indicated in Figure 4. [b] O*−H* and O**−H* bond lengths have the same value.

TABLE 2: Topological Properties (in au) of the Electronic Density at Selected Bond Critical Points for C_2H_6, $C_2H_7^+$, T3, and TS for the Hydrogen Exchange Reaction of Ethane on T3

system	bond	$\rho(\mathbf{r})$	$\nabla^2\rho(\mathbf{r})$	$\lvert\lambda_1\rvert/\lambda_3$	ϵ	$G/\rho(\mathbf{r})$
C_2H_6	C−H	0.2723	−0.8978	1.4226	0.0093	0.1590
	C−C	0.2383	−0.5343	1.2657	0.0000	0.2284
$C_2H_7^+$	C−H	0.2781	−1.0050	1.5796	0.0319	0.1187
	C−C	0.2480	−0.6916	2.2212	0.0121	0.1331
	C−H*	0.2121	−0.3873	4.9777	2.4941	0.6549
	H*−H*	0.2215	−0.5980	3.4965	1.7496	0.1725
T3	O*−H*	0.3540	−2.4864	1.6923	0.0143	0.1839
TS	C−H	0.2683	−0.8641	1.3963	0.0341	0.1681
	C−C	0.2367	−0.5212	1.2568	0.0080	0.2345
	C−H*	0.1617	−0.2791	0.9919	0.3483	0.2461
	O*−H*[a]	0.1154	0.0765	0.4435	0.0120	0.6586

[a] The O*−H* and O**−H* bonds have the same topological properties.

geometric parameters such as the C−C and C−H bond distances and the H−C−H bond angle tends to reinforce the above argument since only minor changes occur during the formation of the TS. However, an appreciable increase of the C−H* bond length and the H*−C−H* bond angle values in the TS with respect to the free carbocation can be observed. Moreover, the O*−H* bond in T3 becomes considerably enlarged when the TS is formed. A new O**−H* bond appears when the TS is formed and it is identical to the O*−H* bond.

The total topology of the TS is consistent with the Poincaré-Hopf relationship,[19] which states that the number of nuclei minus the number of BCPs plus the number of ring CP minus the number of cage CP must be equal to 1 (24 − 24 + 1 − 0 = 1 in the present case).

Table 2 shows the calculated topological properties of the electronic density at some selected BCPs for the species under study. It can be seen that the C−H and C−C bonds in free ethane, free H-ethonium, and the TS can be clearly characterized as covalent bonds according to their topological properties. The C−H* bonds, on the other hand, show a rather smaller value of $\rho(\mathbf{r})$ and a somewhat less negative value of $\nabla^2\rho(\mathbf{r})$ in the TS than in the free H-ethonium ion. Both the $|\lambda_1|/\lambda_3$ and $G/\rho(\mathbf{r})$ relationships are considerably lower in the TS than in the free ion for the C−H* bonds, but their magnitudes are still within the covalent regime.

It is interesting to see that a bond evolved between the H* atoms in free H-ethonium according to the results shown in Table 2 (see also Figure 2). Its topological properties are typical of covalent bonds as it was already observed in other H-carbonium ions.[20] However, no H*−H* bond is found in the

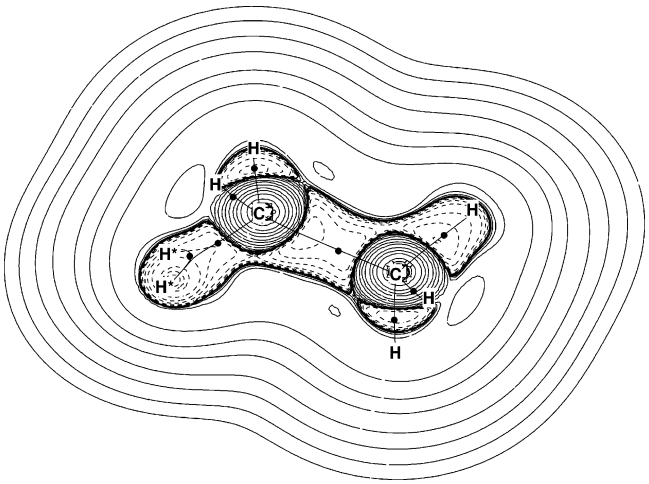

Figure 2. Laplacian of the electronic density of the H-ethonium ion, $C_2H_7^+$. The plane containing the two C atoms and one of the H* atoms is shown. Solid lines represent regions of electronic charge depletion, and dashed lines denote regions of electronic charge concentration. Bond critical points are indicated with circles. The molecular graph is also indicated. The contours of the Laplacian of the electronic density increase and decrease from a zero contour in steps of $\pm2 \times 10^n$, $\pm4 \times 10^n$, and $\pm8 \times 10^n$, with *n* beginning at −3 and increasing by unity. The same set of contours is used in all the figures of the present work.

$C_2H_7^+$ structure in the TS. This important finding indicates that the carbocation structure in the TS is different from that of free H-ethonium.

The large ellipticity values of the C−H* and H*−H* bonds in free H-ethonium indicate a structural instability, probably related to the characteristic three-center, two-electron bond found for this species. On the contrary, the ellipticity of the C−H* bond in the TS is considerably lower than one, showing that the above instability in the free carbocation no longer exists. These facts, already found for the interaction of methane with the T3 cluster,[8] suggest that the zeolite behaves not as a simple counterion in the whole hydrogen exchange process, but it plays an important role enabling a net stabilization of the carbocationic structure.

The O*−H* bond in the T3 cluster shows the typical features of covalent bonds. However, when the TS is formed, the O*−H* and O**−H* bonds exhibit important changes in their topological properties. The electronic density presents a rather small value at the BCP. The Laplacian of the electronic density, $\nabla^2\rho(\mathbf{r})$, shows a small, positive value at the BCP. Moreover, the $|\lambda_1|/\lambda_3$ relationship is now appreciably lower than one and even when the $G/\rho(\mathbf{r})$ relationship is still lower than the unity, it exhibits a considerable increase with respect to the modest value presented in the T3 cluster. All these facts clearly indicate that a closed-shell interaction between a carbocationic structure and a negatively charged T3 cluster occurs when the TS is formed. This result is consistent with the result found for the interaction of methane with a T3 cluster.[8]

Figures 2 and 3 depict the Laplacian of the electronic density for $C_2H_7^+$ and the TS for the hydrogen exchange reaction. The molecular graphs are also indicated in the figures. It is observed in Figure 2 that the H*−H* bond presents a critical point, which is further located in a region of charge concentration. This fact clearly demonstrates that a three-center, two-electron system has evolved in free H-ethonium, as it was indicated before according to the data shown in Table 2. As a consequence of the opening of the H*−C−H* angle in the TS, the electronic density is much less concentrated between those three atoms, and the H*−H* bond is destroyed as can be clearly appreciated

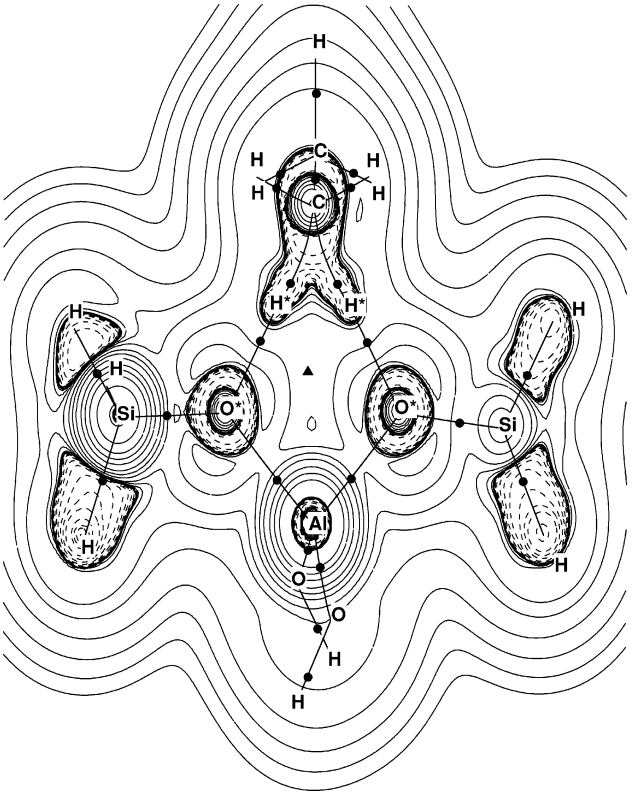

Figure 3. Laplacian of the electronic density of the transition state for the hydrogen exchange reaction. The plane containing the O*, O**, and two H* atoms is shown. Solid lines represent regions of electronic charge depletion, and dashed lines denote regions of electronic charge concentration. Bond critical points and ring critical point are indicated with circles and triangles, respectively. The molecular graph is also indicated.

in Figure 3. These findings allow us to reinforce the argument that in the TS no free H-ethonium exists and that the interaction with the zeolite produces important changes in the carbocation. Also, in Figure 3 the BCPs of both O*−H* and O**−H* bonds are located in a region of charge depletion, a fact that allows us to confirm their ionic nature.

It is finally interesting to stress that the O* and O** atoms in T3 play quite different roles during the interaction with ethane. The O* atom, on one hand, behaves as a Brønsted acid by releasing a hydrogen atom that is bonded to one of the carbon atoms of ethane. On the other hand, the O** atom behaves as a Lewis base by stabilizing a hydrogen atom of ethane through a closed-shell interaction.

Figure 4 shows the optimized geometry of the TS for the dehydrogenation reaction of ethane on a T3 cluster representing a zeolite acid site. It can be seen that the TS seems to be formed by three well-defined fragments, namely, a negatively charged zeolite, a pseudo H_2 molecule, in which the H−H bond distance is slightly larger than the value of 0.74 Å found for the isolated H_2 molecule at the B3LYP/6-31G** level of theory, and a $C_2H_5^+$ carbocation. There is a very important issue related to the ethyl cation, however, that must be considered. Scheme 1 shows the two possible structures for $C_2H_5^+$.

Several experimental and theoretical studies indicate that the nonclassical conformer is the most stable form of the ethyl cation by an amount ranging from 0.8 to 6.3 kcal/mol.[21] Furthermore, it is not clear from those studies whether the classical structure is a local minimum or a transition state. It is evident from Figure 4 that the $C_2H_5^+$ fragment in the TS resembles the classical form of the ethyl cation.

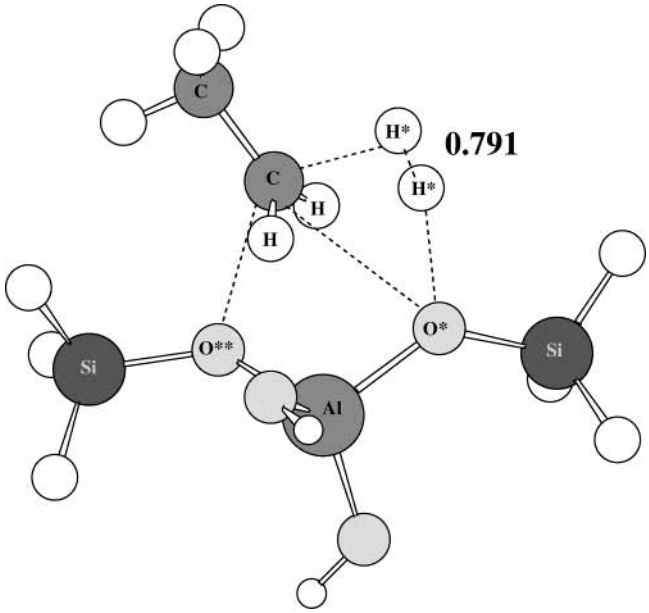

Figure 4. Optimized geometry of the transition state for the dehydrogenation reaction of ethane on a T3 cluster. See Tables 1 and 3 for labels. The H*−H* bond distance is given in Å.

SCHEME 1

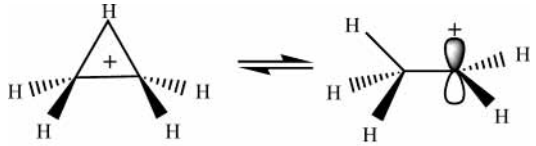

The most important geometric parameters of C_2H_6, the nonclassical form of $C_2H_5^+$, T3, and TS for the dehydrogenation reaction are shown in Table 1. Even though it is not very useful to compare the geometries of the nonclassical form of $C_2H_5^+$ and the classical-like structure found in the TS, the C−C bond distance increases by almost 0.1 Å in the latter. The C−H* bond distance becomes also enlarged by almost 0.5 Å. The C−O* and C−O** bond distances, on the other hand, are very large and asymmetric, the carbon atom being closer to the nonacidic oxygen atom in the T3 fragment. Finally, the O*−H* bond distance in the TS is larger by a factor of 2 with respect to the value in the T3 cluster.

The total topology of this TS is also consistent with the Poincaré-Hopf relationship[19] ($24 - 26 + 3 - 0 = 1$ for the present case, see above for the meaning of the numbers).

Table 3 shows the topological properties of the electronic density calculated at some selected BCPs for the species under consideration for the dehydrogenation reaction. The C−H and C−C bonds in free ethane, the nonclassical form of $C_2H_5^+$, and the TS can be clearly characterized as covalent bonds according to their topological properties. A large ellipticity is exhibited by the C−H* bond in the nonclassical $C_2H_5^+$. This fact suggests an intrinsic instability for those bonds and a tendency to relax to a more stable structure. The topological properties of the shorter C−H* bond in the TS, on the contrary, indicate that it can be properly described as a closed-shell interaction. Even when $G/\rho(\mathbf{r})$ is not greater than the unity for the C−H* bond, it is considerably larger than the values found for those bonds characterized as covalent ones.

The C−O* and C−O** bonds can be clearly classified as closed-shell interactions or ionic bonds according to their topological properties summarized in Table 3. The large

TABLE 3: Topological Properties (in au) of the Electronic Density at Selected Bond Critical Points for C_2H_6, $C_2H_5^+$, T3, and TS for the Dehydrogenation Reaction of Ethane on T3

system	bond	$\rho(\mathbf{r})$	$\nabla^2\rho(\mathbf{r})$	$\lvert\lambda_1\rvert/\lambda_3$	ϵ	$G/\rho(\mathbf{r})$
C_2H_6	C−H	0.2723	−0.8978	1.4226	0.0093	0.1590
	C−C	0.2383	−0.5343	1.2657	0.0000	0.1909
$C_2H_5^+$	C−H	0.2865	−1.0386	1.3823	0.0199	0.0873
	C−C	0.3128	−0.8750	2.0720	0.1984	0.3564
	C−H*	0.1813	−0.2179	1.2812	1.9045	0.3480
T3	O*−H*	0.3540	−2.4864	1.6923	0.0143	0.1839
TS	C−H	0.3006	−0.1347	1.4149	0.0346	0.0858
	C−C	0.2704	−0.6991	1.5507	0.0267	0.2696
	C−H*[a]	0.0530	0.0970	0.2729	0.1233	0.5849
	C−O**	0.0289	0.1044	0.1955	1.0934	0.8304
	C−O*	0.0181	0.0749	0.1389	0.4544	0.9005
	H*−H*[b]	0.2298	−0.8668	1.2313	0.0201	0.0257
	O*−H*	0.0330	0.0978	0.2444	0.0480	0.7424

[a] These values correspond to the shorter C−H* bond, which is indicated in Figure 4. [b] $\rho(\mathbf{r})$ and $\nabla^2\rho(\mathbf{r})$ equal 0.2618 and −1.0614 au, respectively, for isolated H_2 calculated at the B3LYP/6-311++G** level of theory.

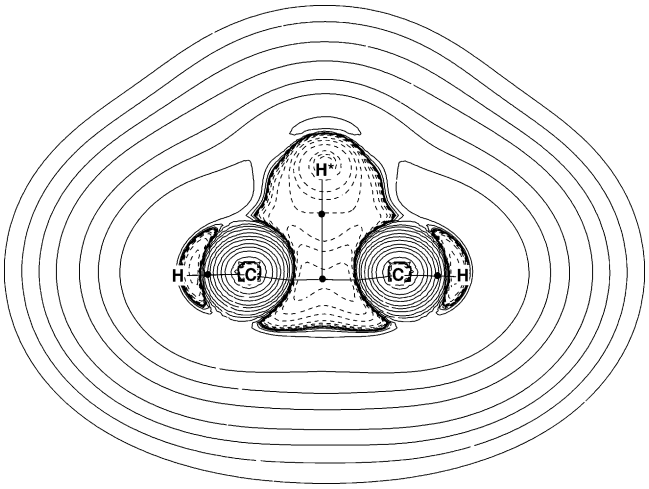

Figure 5. Laplacian of the electronic density of the nonclassical form of the ethyl cation, $C_2H_5^+$. The plane containing the C atoms and the bridge H* atom is shown. Solid lines represent regions of electronic charge depletion, and dashed lines denote regions of electronic charge concentration. Bond critical points are indicated with circles. The molecular graph is also indicated.

ellipticity value presented by C−O** can be thought of as a tendency for that bond to decrease its value when going from the TS to the reaction products.

The O*−H* bond shows quite important changes from the isolated T3 to the TS. The change in its topological properties is consistent with the enlargement underwent by that bond. The topological properties clearly indicate that the O*−H* bond changes from a covalent-like interaction in T3 to a closed-shell one in the TS.

The H*−H* bond exhibits a set of topological properties that allow us to characterize it as a covalent interaction. Furthermore, these magnitudes are not very different from the corresponding values for the isolated H_2 molecule evaluated at the B3LYP/6-311++G** level of theory, see Table 3.

Figures 5 and 6 show the Laplacian of the electronic charge density for the nonclassical form of $C_2H_5^+$ and the TS. It can be seen, first, that the BCP corresponding to the C−H* interactions in the ethyl cation are located in a region of electronic charge concentration, see Figure 5. This finding is consistent with the characterization of that interaction as a shared one. Figure 6 shows that the BCPs corresponding to the C−C, C−H, and H*−H* bonds are found in a region of charge concentration, a fact that allows us to confirm that those bonds are mainly covalent in character. Finally, it can be appreciated in Figure 6 that the BCPs corresponding to the C−O*, C−O**, C−H*, and O*−H* bonds are located in regions of charge depletion, which is the typical behavior shown by closed-shell interactions. All these findings clearly suggest that the TS for the dehydrogenation reaction of ethane on a T3 cluster representing a zeolite acid site can be described as a weak, closed-shell interaction of three fragments, namely, a carbocation resembling the classical form of the ethyl cation, see Scheme 1 above, a negatively charged T3 cluster, and a H_2 pseudomolecule.

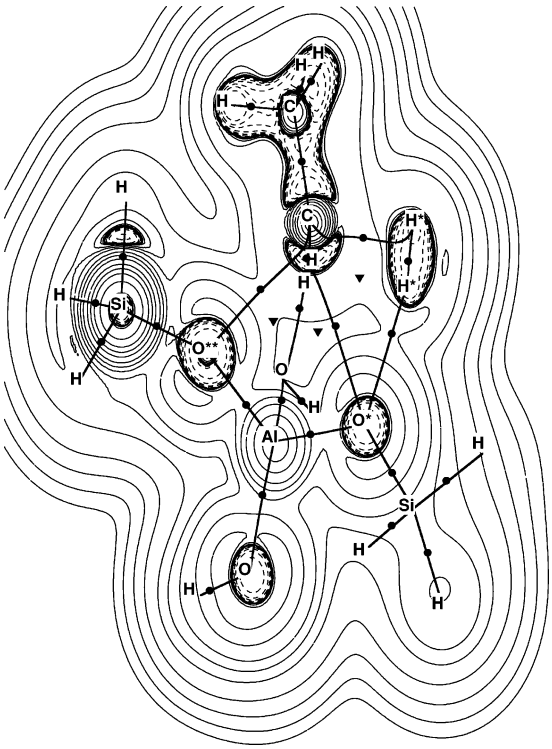

Figure 6. Laplacian of the electronic density of the transition state for the dehydrogenation reaction. The plane containing the C, O*, O**, and two H* atoms is shown. Solid lines represent regions of electronic charge depletion, and dashed lines denote regions of electronic charge concentration. Bond critical points and ring critical points are indicated with circles and triangles, respectively. The molecular graph is also indicated.

Conclusions

A topological study of the transition states of the hydrogen exchange and dehydrogenation reactions of ethane on a zeolite acid site represented by a T3 cluster is presented in this work within the framework of the density functional theory and the atoms-in-molecules method.

The transition state for the hydrogen exchange reaction is formed by a rather ionic interaction between a carbocationic fragment, which resembles the H-ethonium cation $C_2H_7^+$, and a negatively charged T3 cluster. A careful comparison of the topological properties of free H-ethonium and the carbocationic fragment mentioned above allows us to claim that no free $C_2H_7^+$ is present in the transition state. This finding is in line with results reported by other authors. Also, the zeolite plays an important role by reducing some structural instabilities observed in free H-ethonium but absent in the carbocationic fragment in the transition state.

The transition state for the dehydrogenation reaction of ethane on a zeolite acid site is characterized as a weak ionic interaction between three well-defined fragments, namely, an ethyl cation $C_2H_5^+$, a negatively charged T3 cluster, and a H_2 pseudomolecule, in which the H−H distance is only slightly larger than the equilibrium distance in H_2. The cationic fragment found in the transition state presents the so-called classical form of the ethyl cation, which is not the more stable one. The nonclassical form of the ethyl cation, on the other hand, shows a structure in which the fifth hydrogen atom takes part of a three-center, two electron bond together with the two carbon atoms. This is the most stable form of $C_2H_5^+$. Thus, the zeolite acid site plays a significant role in stabilizing a higher-energy form of the $C_2H_5^+$ carbocation in the transition state.

Acknowledgment. The authors acknowledge the Supercomputer Center of SECyT, Argentina, for computational time. N.B.O. thanks SECYT-UNNE for a scholarship. R.P.D. and A.H.J. are members of the Scientific Research Careers of CONICET and CICPBA, Argentina, respectively.

References and Notes

(1) Pines, H. *The Chemistry of Catalytic Hydrocarbon Conversion*; Academic Press: New York, 1981.

(2) Olah, G. A.; Molnar, A. *Hydrocarbon Chemistry*; Wiley-Interscience: New York, 1995.

(3) Blaszkowski, S. R.; van Santen, R. A. *Top. Catal.* **1997**, *4*, 145.

(4) (a) Corma, A.; Miguel, P. J.; Orchiles, V. A. *J. Catal.* **1994**, *145*, 171. (b) Corma, A.; Planelles, J.; Sandoz-Marin, J.; Thomas, F. *J. Catal.* **1985**, *93*, 30. (c) Haag, W. O.; Dessan, R. M. *Proceedings of the 8th International Congress in Catalysis*, Vol. 2; Dechema: Frankfurt an Main, 1984.

(5) Olah, G. A. *Angew. Chem., Int. Ed. Engl.* **1972**, *12*, 173. (b) Olah, G. A.; Prakash, S. K.; Sommer, J. *Superacids*; Wiley-Interscience: New York, 1985.

(6) (a) Haw, J. F.; Richardson, B. R.; Oshiro, I. S.; Lazo, N. D.; Speed, A. J. *J. Am. Chem. Soc.* **1989**, *111*, 2052. (b) Haw, J. F.; Nicholas, J. B.; Xu, T.; Beck, L. W.; Ferguson, D. B. *Acc. Chem. Res.* **1996**, *29*, 259. (c) Sommer, J.; Hauchoumy, M.; Garin, F.; Bartho Meuf, D. *J. Am. Chem. Soc.* **1994**, *116*, 5491. (d) Krannila, H.; Haag, W. O.; Gates, B. C. *J. Catal.* **1992**, *135*, 115. (e) Kwak, B. S.; Sachtler, W. M. H.; Haag, W. O. *J. Catal.* **1994**, *149*, 465.

(7) Esteves, P. M.; Nascimento, M. A. C.; Mota, C. J. A. *J. Phys Chem. B* **1999**, *103*, 10417.

(8) Okulik, N. B.; Pis Diez, R.; Jubert, A. H.; Esteves, P. M.; Mota, C. J. A. *J. Phys. Chem. A* **2001**, *105*, 7079.

(9) Blaszkowski, S. R.; Nascimento, M. A. C.; van Santen, R. A. *J. Phys. Chem.* **1996**, *100*, 3463.

(10) van Santen, R. A.; Kramer, G. J. *Chem. Rev.* **1995**, *95*, 637.

(11) (a) Hohenberg, P.; Kohn, W. *Phys. Rev.* **1964**, *136B*, 864. (b) Kohn, W.; Sham, L. J. *Phys. Rev.* **1965**, *140A*, 1133. (c) Parr, R. G.; Yang, W. *Density Functional Theory of Atoms and Molecules;* Oxford University Press: Oxford, 1989.

(12) (a) Bader, R. F. W. *Atoms in Molecules. A Quantum Theory*; Clarendon: Oxford, 1990. (b) Popelier, P. L. A. *Atoms in Molecules. An Introduction;* Pearson Education: Harlow, U.K., 1999.

(13) Frisch, M. J.; Trucks, G. W.; Schlegel, H. B.; Gill, P. M. W.; Johnson, B. G.; Robb, M. A.; Cheeseman, J. R.; Keith, T.; Petersson, G. A.; Montgomery, J. A.; Raghavachari, K.; Al-Laham, M. A.; Zakrzewski, V. G.; Ortiz, J. V.; Foresman, J. B.; Cioslowski, J.; Stefanov, B. B.; Nanayakkara, A.; Challacombe, M.; Peng, C. Y.; Ayala, P. Y.; Chen, W.; Wong, M. W.; Andres, J. L.; Replogle, E. S.; Gomperts, R.; Martin, R. L.; Fox, D. J.; Binkley, J. S.; Defrees, D. J.; Baker, J.; Stewart, J. P.; Head-Gordon, M.; Gonzalez, C.; Pople, J. A. *Gaussian 94*, Revision E.1; Gaussian, Inc.; Pittsburgh, PA, 1995.

(14) Becke, A. D. *J. Chem. Phys.* **1993**, *98*, 5648.

(15) Lee, C.; Yang, W.; Parr, R. G. *Phys. Rev. B* **1988**, *37*, 785.

(16) (a) Baker, J. *J. Comput. Chem.* **1986**, *7*, 385. (b) Baker, J. *J. Comput. Chem.* **1987**, *8*, 563.

(17) Blieger-Konig, F. W.; Bader, R. F. W.; Tang, T.-H. *J. Comput. Chem.* **1982**, *3*, 317.

(18) (a) Kohler, H. J.; Lischka, H. H. *Chem. Phys. Lett.* **1978**, *58*, 175. (b) Cremer, D.; Kraka, E.; Slee, T. S.; Bader, R. F. W.; Lau, C. D. H.; Nguyen-Dang, T. T.; MacDougall, P. J. *J. Am. Chem. Soc.* **1983**, *105*, 5069.

(19) Collard, K.; Hall, G. G. *Int. J. Quantum Chem.* **1977**, *12*, 623.

(20) (a) Okulik, N. B.; Peruchena, N.; Esteves, P. M.; Mota, C. J. A.; Jubert, A. H. *J. Phys. Chem. A* **1999**, *103*, 8491. (b) Okulik, N. B.; Peruchena, N.; Esteves, P. M.; Mota, C. J. A.; Jubert, A. H. *J. Phys. Chem. A* **2000**, *104*, 7586. (c) Okulik, N. B.; Sosa, L.; Esteves, P. M.; Mota, C. J. A.; Jubert, A. H.; Peruchena, N. *J. Phys. Chem. A* **2002**, *106*, 1584.

(21) Hiraoka, K.; Shoda, T.; Kudaka, I.; Fujimaki, S.; Mizuse, S.; Yamabe, S.; Wasada, H.; Wasada-Tsutsui, Y. *J. Phys. Chem. A* **2003**, *107*, 775.